Dalton Transactions

Accepted Manuscript

ROYAL SOCIETY OF CHEMISTRY

www.rsc.org/dalton

Dalton Transactions

COMMUNICATION

Competing Ferro- and Antiferromagnetic Interactions in a Hexagonal Bipyramidal Nickel Thiolate Cluster

Received 00th January 20xx,
Accepted 00th January 20xx

DOI: 10.1039/x0xx00000x

www.rsc.org/chemcomm

Tomohiko Hamaguchi,[a] Michael D. Doud,[b] Jeremy Hilgar,[b] Jeffrey D. Rinehart,[b] and Clifford P. Kubiak*[,b]

A new hexagonal bipyramidal Ni_8 cluster is reported and its magnetic behaviour is analyzed. The molecular structure consists of a hexagonal wheel capped by two additional apical Ni^{2+} ions. This structure supports ferromagnetic superexchange interactions between adjacent Ni^{2+} ions in the wheel and an antiferromagnetic superexchange interaction between the wheel and apical Ni^{2+} ions.

Molecular inorganic cluster chemistry offers a unique platform for the investigation of the nature and strength of magnetic superexchange interactions. The structural complexity and tunability of clusters allows for the systematic determination of the effects of metal, ligand, oxidation state, coordination number, and geometry on magnetic exchange and anisotropy. Understanding these properties rigorously leads to an increase in the knowledge-base for specifically designed functional magnetic materials. Of specific utility are closed-loop wheel-type complexes due to their tendency to possess large-spin ground states. Many Ni^{2+} clusters have been reported previously,[1-4] but wheel-type hexanuclear Ni^{2+} complexes[5-15] (Scheme 1(a)) are particularly attractive complexes due to their tunability of the number of Ni^{2+} ions. The hexanuclear Ni^{2+} complexes can contain sufficient internal void space to accept a guest molecule.[16-19] In some cases, this void space is occupied by an additional Ni^{2+} ion, forming the Anderson-type heptanuclear structure (Scheme 1(b)).[20-26]

(a) (b) (c)

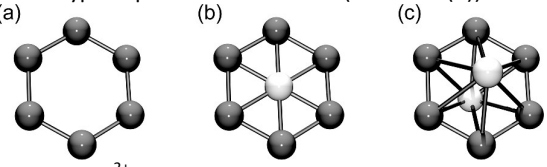

Insertion of Ni^{2+} makes a great impact for their magnetic behavior. Increasing the nuclearity to eight while maintaining the same motif leads to the α-Mo_8O_{26} cluster type, wherein the hexagonal metal wheel is bi-capped with apical metal ions (Scheme 1(c)).[27-31] Humphrey et al.[29] have reported the α-Mo_8O_{26} cluster type with M_2Ni_6 (M = K, Rb, Cs); however, no example of a homonuclear Ni-based α-Mo_8O_{26} type cluster has yet been reported. In this work, we report a new octanuclear Ni cluster $[\{Ni(CH_3CN)_3\}_2\{Ni(\mu\text{-}2\text{-}pyS)(\mu_3\text{-}2\text{-}pyS)\}_6](PF_6)_4$ (**1**) (2-pyS = 2-mercaptopyridinate) and analyze its physical and magnetic structure through X-ray crystallography and SQUID magnetometry, respectively.

The synthesis of **1** is accomplished through a spontaneous self-assembly reaction of $[Ni(H_2O)_6](BF_4)_2$ with 2-mercaptopyridine. Specifically, a mixture of 2-mercaptopyridine in CH_2Cl_2 and $[Ni(H_2O)_6](BF_4)_2$ in CH_3CN (mole ratio of 10 : 1) yields a dark green-yellow solution. Crude sample was obtained as dark green-yellow solid by evacuation of the solution. Purification by recrystallization from vapor diffusion of 2-propanol into an CH_3CN solution containing the product and excess NH_4PF_6 led to isolation of deep brown cubic crystals determined by X-ray crystallographic analysis to be **1** (Fig. 1(a)). ‡ These crystals were also characterized by elemental analysis (in the ESI) and powder X-ray diffraction (Fig. S1 in the ESI), and were used for all measurements.

As shown in Fig. 1(b), the cluster has eight Ni^{2+} ions that are classified into two types. One type of Ni^{2+} ion is arranged hexagonally in a nearly planar arrangement, and the other is mounted above and below the plane. Six Ni^{2+} ions (Ni1, Ni2, Ni3, Ni1*, Ni2*, and Ni3*) are of the first type (hereafter referred to as "planar" nickel), and two Ni^{2+} ions (Ni4 and Ni4*) are of the latter type (hereafter referred to as "capping" nickel). The six planar Ni^{2+} ions show a maximum deviation from planarity of 0.172 Å. Each Ni^{2+} ion is ligated through two monodentate κS-2-pyS and two bidentate $\kappa N,S$-2-pyS units. Adjacent planar Ni^{2+} ions are doubly bridged by two sulfur atoms of 2-pyS ligands. Due to the small bite angle of 2-pyS ligand (~68.8°), these Ni^{2+} centers display a distorted octahedral structure. The average distance between adjacent

[a] Department of Chemistry, Faculty of Science, Fukuoka University, 8-19-1 Nanakuma, Jonan-ku, Fukuoka 814-0180, Japan
[b] Department of Chemistry and Biochemistry, University of California – San Diego, 9500 Gilman Drive, Mail Code 0358, La Jolla, CA 92093-0358, USA
E-mail : ckubiak@ucsd.edu

† Electronic Supplementary Information (ESI) available: detailed information of instrumentation, X-ray study, magnetic study and synthesis. See DOI: 10.1039/x0xx00000x

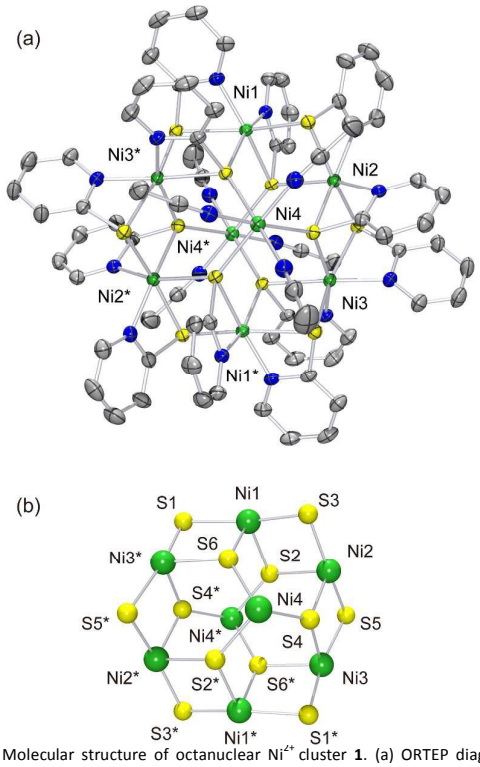

Figure 1. Molecular structure of octanuclear Ni^{2+} cluster **1**. (a) ORTEP diagram with counter anions and hydrogen atoms omitted for clarity. The symmetry operator (½−x, ½+y, ½−z) is used to generate the equivalent atoms marked with an asterisk. Green, gray, blue, and yellow ellipsoids represent Ni, C, N, and S, respectively. (b) Structural core demonstrating important bridging interactions that facilitate magnetic coupling and the approximate 3-fold symmetry about the axis defined by Ni4 and Ni4*.

planar Ni^{2+} centers is 3.44 Å, indicating a lack of metal-metal bonding. The separation between Ni^{2+} centers is longer than that of similar M_1Ni_6 wheel-type nickel clusters[20-26] and Ni_6 wheel-type nickel clusters coordinated by thiolate[10-15] but is almost the same as in previously observed M_2Ni_6 complexes.[29] The average Ni–S bond length and average Ni–S–Ni bond angle is 2.46 Å and 88.9°, respectively. Heptanuclear Ni_1Ni_6 wheel-type clusters typically have a suitable void space for one atom at center of the Ni_6 wheel. In the case of **1**, however, two additional Ni^{2+} ions are coordinated to three S atoms above and below the Ni_6 wheel plane, possibly due to the steric bulk of S atom compared to O atom. Each capping Ni^{2+} ion has three coordinated CH_3CN molecules to complete its octahedral coordination sphere. The average planar-to-capping Ni···Ni separation is 4.50 Å, much longer than adjacent Ni···Ni distances in the plane. Average capping Ni-S bond lengths and Ni(planar)-S-Ni(capping) bond angle are 2.49 Å and 131°, respectively.

The new nickel structural configuration observed for **1** encouraged scrutiny of the magnetic structure it engendered. Therefore, we collected temperature dependent magnetic susceptibility data to determine the nature and magnitude of intracluster magnetic coupling (Fig. 2). The magnetic susceptibility times temperature (χ_mT) value at 300 K was 6.88 emu K mol^{-1}, significantly smaller than the expected value for eight uncoupled Ni^{2+} atoms (8.82 cm^3 K mol^{-1}, g = 2.1), implying a significant influence of antiferromagnetic coupling, even at

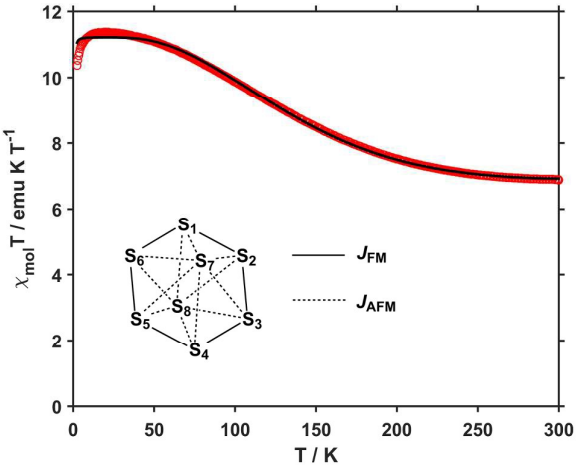

Figure 2. Plot of χ_MT vs. T. The solid line represents a fit to the data using the Hamiltonian described in Eq. 1 (J_{FM} = 12.9 cm^{-1}, J_{AFM} = −30.7 cm^{-1}, g = 2.1.) Inset: Superexchange model displaying the ferromagnetic and antiferromagnetic exchange pathways coupling planar and capping Ni^{2+} ions.

ambient temperature. Upon cooling, χ_mT increases gradually and eventually plateaus near 11 cm^3 K mol^{-1} at 25 K. Below 15 K, χ_mT decreases to 10.4 cm^3 K mol^{-1} at 2 K. This temperature dependence implicates multiple exchange pathways and is consistent with the two types of Ni^{2+} ion present: planar and capping. With the crystallographic coordinates as a guide, we constructed a Hamiltonian described by two exchange pathways: one accounting for magnetic coupling amongst the six planar Ni^{2+} ions and one accounting for magnetic coupling amongst the six planar Ni^{2+} ions and one accounting for the coupling between the planar and capping Ni^{2+} ions (inset to Fig. 2 and Eq. 1).

$$\hat{H} = -2J_{\mathrm{FM}}\left[\sum_{i=1}^{5}\hat{S}_i \bullet \hat{S}_{i+1} + \hat{S}_6 \bullet \hat{S}_1\right] -2J_{\mathrm{AFM}}\sum_{i=1}^{6}\sum_{j=7}^{8}\hat{S}_i \bullet \hat{S}_j + g\mu_B\sum_{i=1}^{8}\vec{B} \bullet \hat{S}_i \qquad [1]$$

The magnetic analysis program *PHI*[32] was employed to fit χ_mT vs. T. Parameters of the best-fit were J_{FM} = 12.9 cm^{-1}, J_{AFM} = −30.7 cm^{-1}, g = 2.1. This result indicates that (1) a ferromagnetic superexchange interaction appears between adjacent planar Ni^{2+} atoms and (2) an antiferromagnetic superexchange interaction appears between the planar and capping Ni^{2+} ions. This behavior is similar to heptanuclear Ni^{2+} complexes. The stronger antiferromagnetic interaction is responsible for the lowering of the room temperature moment while the weaker ferromagnetic interaction leads to the rise at lower temperatures. The antiferromagnetic interaction between the planar (S = 6) and apical (S = 2) sub-units leads to a well isolated S = 4 ground state indicated by the plateau at low temperatures. The nature of the interactions can be further rationalized by orbital interactions dictated by the superexchange bridging angles as described by the

Goodenough-Kanamori rules.[33] An empirical generalization of Ni–X–Ni exchange coupling interactions based on their respective bond angles have been presented previously.[34] To summarize, bond angles of 90 ± 8° have been shown to result in a ferromagnetic coupling, with angles closer to 90° typically

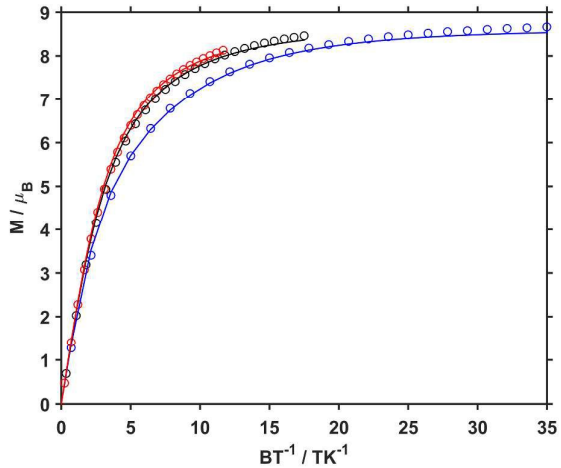

Figure 3. Plot of *M* vs. *B*/*T*. The solid lines represent a fit to the data at 2.00 K (blue), 4.00 K (black), and 6.00 K (red) using the Hamiltonian described in Eq. 2 ($|D| = 0.35$ cm^{-1}, $g = 2.2$.)

resulting in stronger interactions. Coupling between Ni^{2+} centers with bond angles outside this range lead to an antiferromagnetic interaction. The magnitudes of the coupling parameters reported herein are typical of Ni^{2+} centers bridged by sulfur atoms reported elsewhere.[35]

It is evident from the $\chi_M T$ vs. T data that an additional parameter is necessary to correctly model the lowest temperature data. The observed drop in $\chi_M T$ below 15 K far exceeds the expected contribution from the Zeeman effect and is therefore likely due to magnetic anisotropy. To better understand this effect, the field dependence of the magnetization was measured at very low temperature (Fig. 3). These data represent magnetic properties arising from the isolated $S = 4$ ground state and can be used to approximate the second order axial zero-field splitting parameter, D. We fit these data under the giant spin approximation using a Hamiltonian with a single axial anisotropy term (Eq. 2).

$$\hat{H} = D\left[\hat{S}_z^2 - S(S+1)/3\right] + g\mu_B \vec{B} \bullet \hat{S} \qquad [2]$$

MagProp, a sub-routine of the Data Analysis and Visualization Environment[36], was used to fit the variable-temperature magnetization data and yielded the parameters of best fit $|D| = 0.35$ cm^{-1} and $g = 2.2$. The small anisotropy constant is consistent with Ni^{2+} ions in an octahedral environment, as well as for high-nuclearity transition-metal clusters in general. Using these data and the fact that we have an $S = 4$ ground state, a simple calculation can estimate the possible energy barrier ($U_{eff} = S^2|D|$) for single-molecule magnetism in **1**. If we assume a negative axial anisotropy, an energy barrier of $U_{eff} = 5.6$ cm^{-1} is expected; however, AC magnetic susceptibility at switching frequencies up to 1000 Hz show no out-of-phase susceptibility at 2 K, indicating that either D is positive or the thermal barrier is being shortcut by other relaxation processes.

Herein we have presented the structural and magnetic analysis of a new topology of octanuclear nickel cluster. The addition of two capping Ni^{2+} ions to the planar hexagonal motif is deleterious to the overall magnetic moment, due to introduction of a strong antiferromagnetic superexchange pathway. These opposing interactions lead to a net $S = 4$ ground state that is largely magnetically isotropic.

We gratefully acknowledge NSF (CHE-1145893 and CHE-1461632) for support, and Dr. Curtis Moore and Prof. Arnold Rheingold for X-ray crystallographic support.

Notes and references

‡ X-ray crystallographic data. $C_{72}H_{66}N_{18}Ni_8S_{12}P_4F_{24}$, Mw = 2617.6 g/mol, 0.05 × 0.05 × 0.10 mm^3, monoclinic, $P2_1/n$, a = 13.9583(3) Å, b = 22.5215(5) Å, c = 15.3686(4) Å, β = 92.3771(13) °, V = 4827.1(2) Å^3, Z = 2, D_{calc} = 1.801 g/cm^3, μ = 1.949 mm^{-1}, Mo Kα radiation (λ = 0.71070 Å), T = 100 K, $2\theta_{max}$ = 50.66°, number of measured reflections: 39258, number of independent reflections: 8804, R_{int} = 0.021, $R_1(I>2\sigma(I))$ = 0.0366, $wR_2(I>2\sigma(I))$ = 0.1001, Goodness-of-fit on F^2: 1.055, CCDC-1416907.

1. S. T. Ochsenbein, M. Murrie, E. Rusanov, H. Stoeckli-Evans, C. Sekine and H. U. Güdel, *Inorg. Chem.*, 2002, **41**, 5133-5140.
2. M. Murrie, D. Biner, H. Stoeckli-Evans and H. U. Gudel, *Chem. Commun.*, 2003, DOI: 10.1039/B210327C, 230-231.
3. A. Escuer, J. Esteban and O. Roubeau, *Inorg. Chem.*, 2011, **50**, 8893-8901.
4. H. Jiang, T. Sheng, S. Bai, S. Hu, X. Wang, R. Fu, P. Yu and X. Wu, *Inorg. Chem.*, 2013, **52**, 12305-12307.
5. S. Zhang, L. Zhen, B. Xu, R. Inglis, K. Li, W. Chen, Y. Zhang, K. F. Konidaris, S. P. Perlepes, E. K. Brechin and Y. Li, *Dalton Trans.*, 2010, **39**, 3563-3571.
6. B. Sun, X. Chen, Z. Li, L. Zhang and Q. Zhao, *New J. Chem.*, 2010, **34**, 190-192.
7. Z. Zhao, B. Zhou, S. Zheng, Z. Su and C. Wang, *Inorg. Chim. Acta*, 2009, **362**, 5038-5042.
8. I. G. Fomina, G. G. Aleksandrov, Z. V. Dobrokhotova, O. Y. Proshenkina, M. A. Kiskin, Y. A. Velikodnyi, V. N. Ikorskii, V. M. Novotortsev and I. L. Eremenko, *Russ. Chem. Bull.*, 2006, **55**, 1909-1919.
9. G. E. Lewis and C. S. Kraihanzel, *Inorg. Chem.*, 1983, **22**, 2895-2899.
10. H. N. Kagalwala, E. Gottlieb, G. Li, T. Li, R. Jin and S. Bernhard, *Inorg. Chem.*, 2013, **52**, 9094-9101.
11. C. Tan, M. Jin, X. Ma, Q. Zhu, Y. Huang, Y. Wang, S. Hu, T. Sheng and X. Wu, *Dalton Trans.*, 2012, **41**, 8472-8476.
12. R. Angamuthu, H. Kooijman, M. Lutz, A. L. Spek and E. Bouwman, *Dalton Trans.*, 2007, DOI: 10.1039/B713668B, 4641-4643.
13. C. Zhang, S. Takada, M. Kölzer, T. Matsumoto and K. Tatsumi, *Angew. Chem. Int. Ed.*, 2006, **45**, 3768-3772.
14. F.-F. Jian, K. Jiao, Y. Li, P.-S. Zhao and L.-D. Lu, *Angew. Chem. Int. Ed.*, 2003, **42**, 5722-5724.
15. A. H. Mahmoudkhani and V. Langer, *Polyhedron*, 1999, **18**, 3407-3410.
16. A. N. Georgopoulou, C. P. Raptopoulou, V. Psycharis, R. Ballesteros, B. Abarca and A. K. Boudalis, *Inorg. Chem.*, 2009, **48**, 3167-3176.
17. M.-L. Tong, M. Monfort, J. M. C. Juan, X.-M. Chen, X.-H. Bu, M. Ohba and S. Kitagawa, *Chem. Commun.*, 2005, DOI: 10.1039/B415431B, 233-235.

18. G. Gavioli, R. Battistuzzi, P. Santi, C. Zucchi, G. Pályi, G. Pályi, R. Ugo, A. Vizi-Orosz, O. I. Shchegolikhina, Y. A. Pozdniakova, S. V. Lindeman and A. A. Zhdanov, *J. Organomet. Chem.*, 1995, **485**, 257-266.
19. A. Cornia, A. C. Fabretti, D. Gatteschi, G. Palyi, E. Rentschler, O. I. Shchegolikhina and A. A. Zhdanov, *Inorg. Chem.*, 1995, **34**, 5383-5387.
20. C. Ding, C. Gao, S. Ng, B. Wang and Y. Xie, *Chem. Eur. J.*, 2013, **19**, 9961-9972.
21. S. H. Zhang, N. Li, C. M. Ge, C. Feng and L. F. Ma, *Dalton Trans*, 2011, **40**, 3000-3007.
22. L. Q. Wei, K. Zhang, Y. C. Feng, Y. H. Wang, M. H. Zeng and M. Kurmoo, *Inorg. Chem.*, 2011, **50**, 7274-7283.
23. J. Zhang, P. Teo, R. Pattacini, A. Kermagoret, R. Welter, G. Rogez, T. S. Hor and P. Braunstein, *Angew. Chem. Int. Ed.*, 2010, **49**, 4443-4446.
24. S. T. Meally, C. McDonald, G. Karotsis, G. S. Papaefstathiou, E. K. Brechin, P. W. Dunne, P. McArdle, N. P. Power and L. F. Jones, *Dalton Trans.*, 2010, **39**, 4809-4816.
25. S. T. Meally, G. Karotsis, E. K. Brechin, G. S. Papaefstathiou, P. W. Dunne, P. McArdle and L. F. Jones, *CrystEngComm*, 2010, **12**, 59-63.
26. W. L. Leong and J. J. Vittal, *New J. Chem.*, 2010, **34**, 2145-2152.
27. Z.-C. Yue, H.-J. Du, L. Li, W.-L. Zhang, Y.-Y. Niu and H.-W. Hou, *Inorg. Chim. Acta*, 2014, **410**, 136-143.
28. D. S. Nesterov, J. Jezierska, O. V. Nesterova, A. J. Pombeiro and A. Ozarowski, *Chem. Commun.*, 2014, **50**, 3431-3434.
29. S. M. Humphrey, R. A. Mole, M. McPartlin, E. J. L. McInnes and P. T. Wood, *Inorg. Chem.*, 2005, **44**, 5981-5983.
30. K. Nomiya, H. Yokoyama, R. Noguchi and K. Machida, *Chem. Lett.*, 2002, **31**, 922-923.
31. R. W. Saalfrank, I. Bernt and F. Hampel, *Angew. Chem. Int. Ed.*, 2001, **40**, 1700-1703.
32. N. F. Chilton, R. P. Anderson, L. D. Turner, A. Soncini and K. S. Murray, *J. Comput. Chem.*, 2013, **34**, 1164-1175.
33. O. Kahn, *Molecular Magnetism*, Wiley-VCH, New York, 1993.
34. Y. Journaux, T. Glaser, G. Steinfeld, V. Lozan and B. Kersting, *Dalton Trans.*, 2006, DOI: 10.1039/B513717A, 1738-1748.
35. T. Beissel, F. Birkelbach, E. Bill, T. Glaser, F. Kesting, C. Krebs, T. Weyhermüller, K. Wieghardt, C. Butzlaff and A. X. Trautwein, *J. Am. Chem. Soc.*, 1996, **118**, 12376-12390.
36. R. T. Azuah, L. R. Kneller, Y. Qiu, P. L. W. Tregenna-Piggott, C. M. Brown, J. R. D. Copley and R. M. Dimeo, *J. Res. Natl. Inst. Stan. Technol.*, 2009, **114**, 341-358.

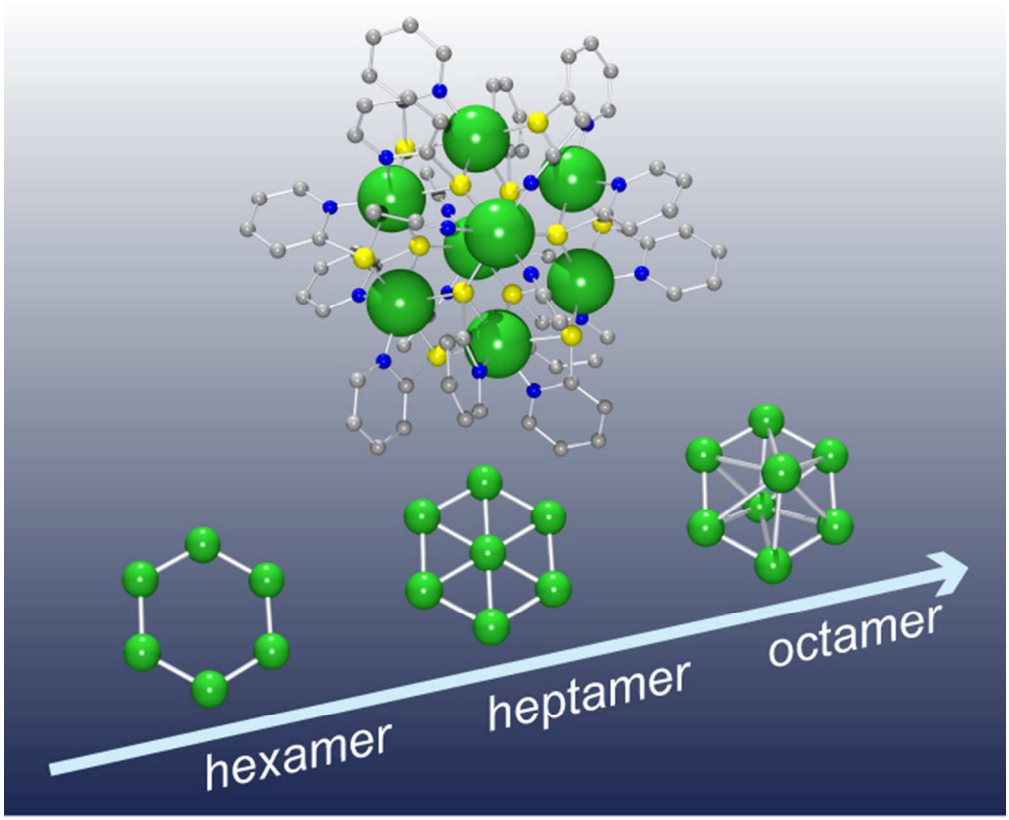

57x46mm (300 x 300 DPI)